Supporting Information

Chaves-Sanjuan et al. 10.1073/pnas.1407610111

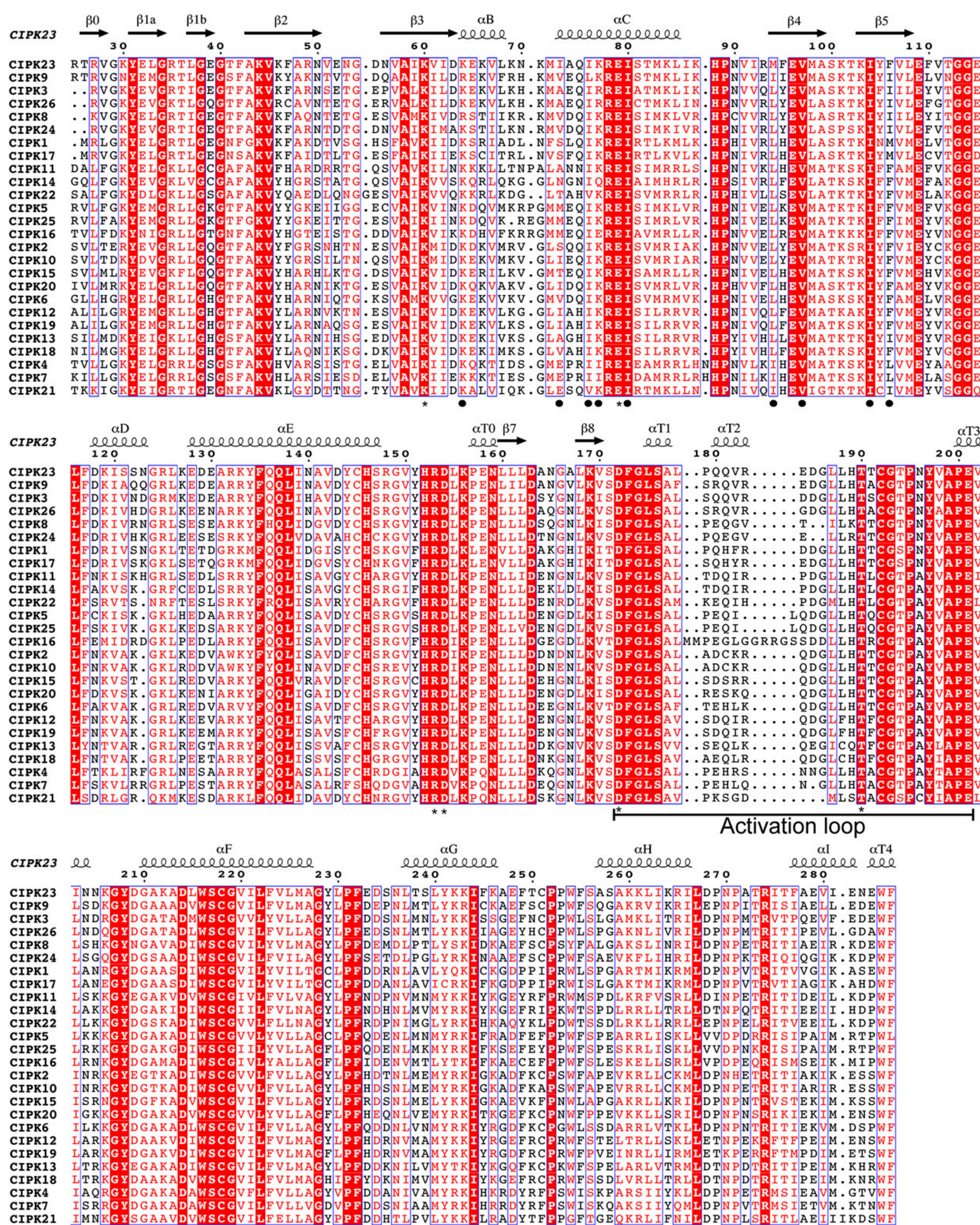

Fig. S1. Alignment comparing the amino acid sequences of the catalytic domain of CIPKs (1). The positions of the CIPK23ΔC T190D secondary structure elements determined from the crystal structure are shown above the sequences (2). Residues are colored according to their conservation (3). Catalytically relevant residues and residues involved in CHAPS binding are highlighted with a black dot and with an asterisk, respectively.

1. Thompson JD, Gibson TJ, Higgins DG (2002) Multiple sequence alignment using ClustalW and ClustalX. *Curr Protoc Bioinformatics* Chapter 2:Unit 2.3.
2. Kabsch W, Sander C (1983) Dictionary of protein secondary structure: pattern recognition of hydrogen-bonded and geometrical features. *Biopolymers* 22(12):2577–2637.
3. Gouet P, Courcelle E, Stuart DI, Métoz F (1999) ESPript: Analysis of multiple sequence alignments in PostScript. *Bioinformatics* 15(4):305–308.

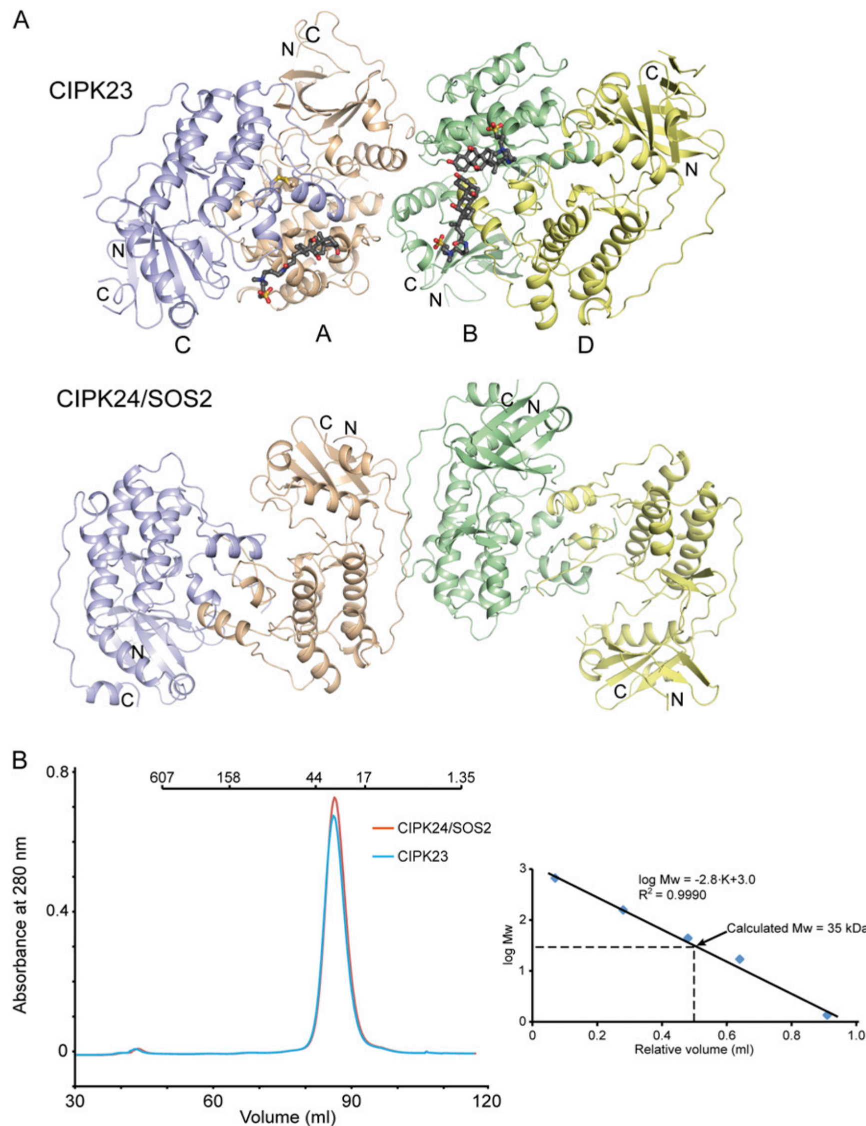

Fig. S2. (*A*) CIPK23ΔC T190D and CIPK24/SOS2ΔC T168D crystal packing interactions within the asymmetric unit. A ribbon representation of those molecules constituting the asymmetric unit. The Cα rmsd between the different molecules found in the asymmetric unit ranges from 0.7 to 1.0 Å in the case of ΔC, and from 0.5 to 0.7 Å in CIPK24/SOS2ΔC T168D (1). The residues forming a disulfide bridge between equivalent CIPK23 Cys192 of monomers within the asymmetric unit are displayed in a stick representation. Formation of the disulfide bridge is likely a crystallization artifact since increasing the TCEP concentration in the crystallization drop from 0.25 mM to 2.5 mM inhibits CIPK23ΔC T190D crystallization. A topologically equivalent disulfide bound was observed in Snf1 MARK2 kinase with no biological implications (2). (*B*) The oligometric state of CIPK23ΔC T190D (red) and CIPK24/SOS2ΔC T168D (blue) in solution as show by gel filtration chromatography.

1. Emsley P, Lohkamp B, Scott WG, Cowtan K (2010) Features and development of Coot. *Acta Crystallogr D Biol Crystallogr* 66(Pt 4):486–501.
2. Panneerselvam S, Marx A, Mandelkow EM, Mandelkow E (2006) Structure of the catalytic and ubiquitin-associated domains of the protein kinase MARK/Par-1. *Structure* 14(2):173–183.

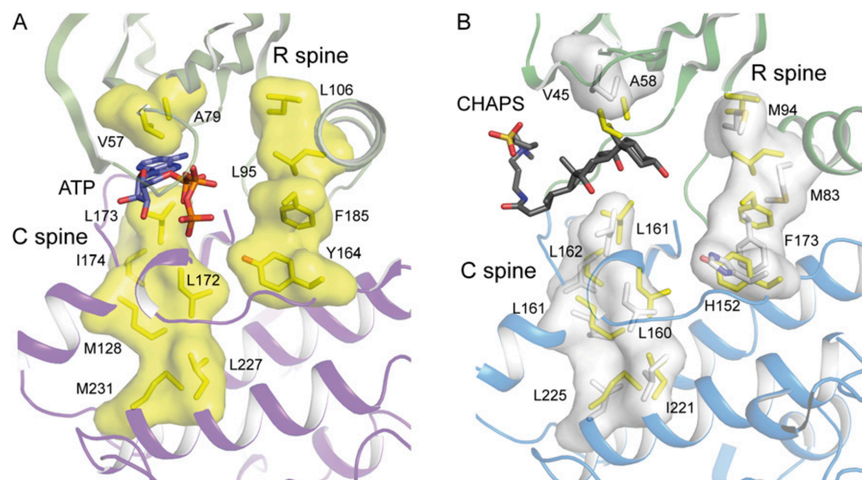

Fig. S3. The local spatial pattern alignment have been efficiently used to identify two structural motives composed by spines of hydrophobic residues that are conserved in active kinases but not in the inactive ones (1). One of them is the regulatory spine or R spine, which consist in four residues, two from the N lobe and two from the C lobe. The second spine is the catalytic spine or C spine. It is conformed by two residues from the N lobe, the adenine ring from the ATP, and other six residues from the C lobe. (*A*) A molecular surface representation of the C and R spines of the PKA active kinase (PDB ID code: 1ATP). Residues forming the spines are represented as yellow sticks. (*B*) A molecular surface representation of the topologically equivalent spines of CIPK23. Residues forming the spines are displayed as white sticks and overlaid to those forming the PKA spines. According to the inactive state of CIPK23, the residues are not aligned along the two spines. Met83 at αC breaks the R spine because it is not stacked between residues Met94 and F173. C spine is broken at the ATP binding site because of the presence of a CHAPS molecule and the open conformation of the N lobe with respect to the C lobe.

1. Taylor SS, Kornev AP (2011) Protein kinases: Evolution of dynamic regulatory proteins. *Trends Biochem Sci* 36(2):65–77.

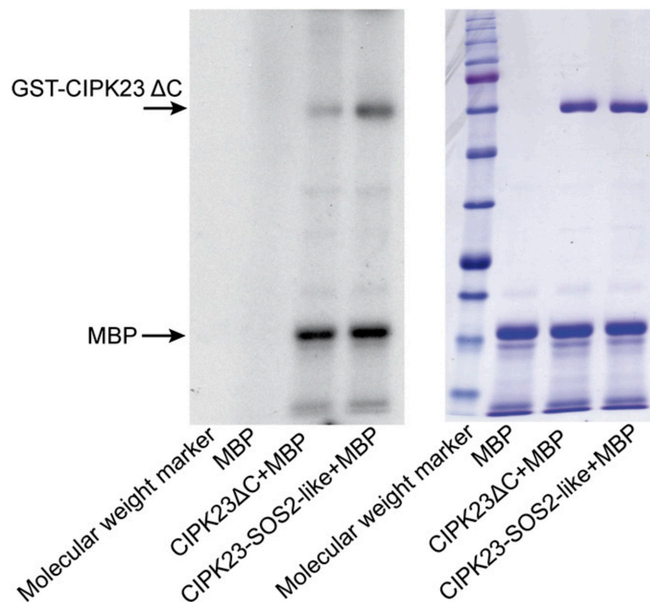

Fig. S4. A mutant CIPK23 protein converted into a CIPK24/SOS2-like protein by the replacement of the CIPK23 activation loop with that of CIPK24/SOS2 displays enhanced autophosphorylation kinase activity. The autoradiograph showing the CIPK23ΔC and CIPK23-SOS2–like in vitro kinase assay is shown (*Left*). The reaction mixture contains myelin basic protein (MBP) as substrate in the presence of [^{32}P]ATP. (*Right*) The Coomassie-stained gel is shown. CIPK23-SOS2–like construct was prepared by the mutation of Val182Gly Arg183Val and His189Arg and the deletion of Asp185 and Gly186. The proteins were purified from *S. cerevisiae* as GST fusions because CIPK23-SOS2-Like protein was insoluble when expressed in *E. coli*.

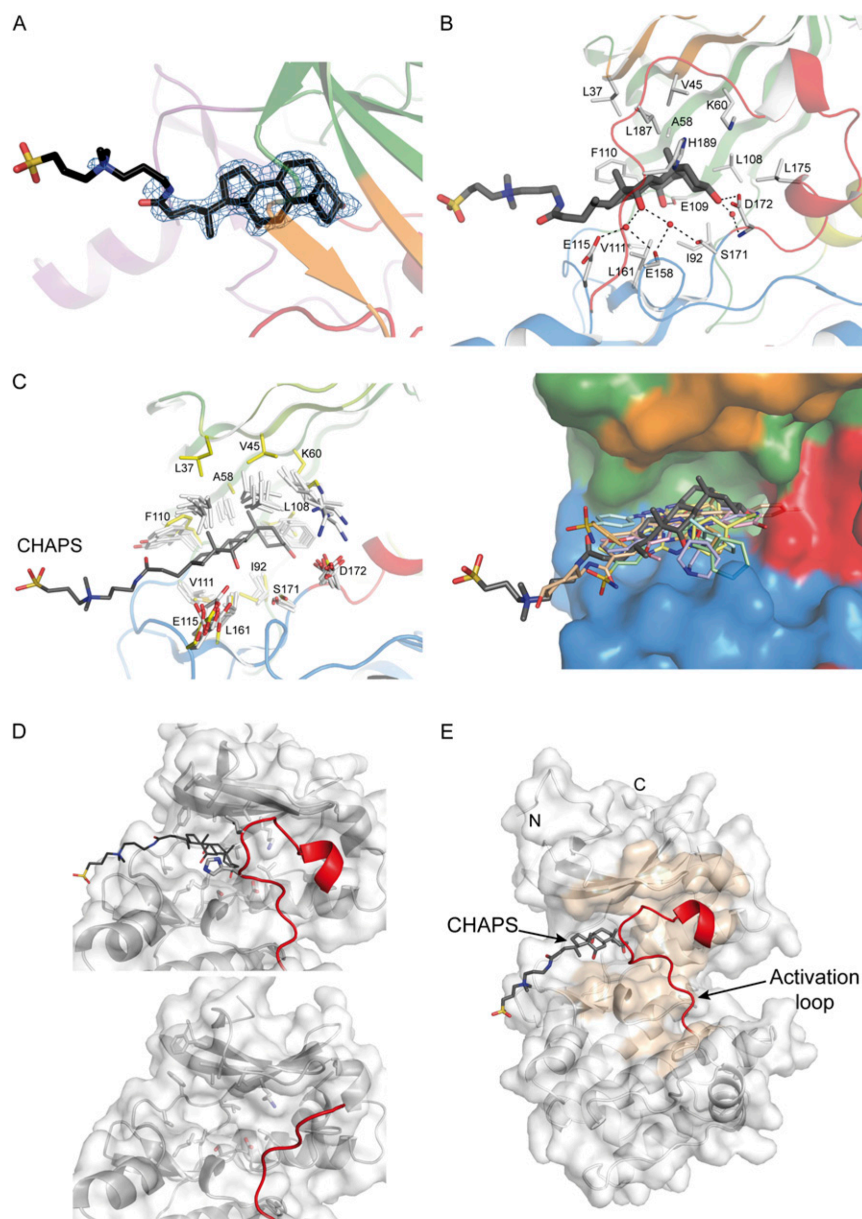

Fig. S5. The CHAPS molecule at ATP binding pocket. (*A*) A section of the simulated annealed omit Fo-Fc electron density map at the ATP binding pocket defines the cholate ring of a CHAPS molecule. (*B*) A representation of the pattern of Interactions between the CHAPS molecule and CIPK23ΔC T190D. The interacting residues are labeled and displayed in a stick representation. Hydrogen bonds are displayed as dashed lines. Water molecules are represented as red spheres. (*C*) Superimpositions of the closest structures to CIPK23ΔC T190D at the ATP binding pocket. (*C*, *Left*) Overlay of the binding sites. (*C*, *Right*) Overlay of the bounded ligands (PDB ID codes: 3BHH, 1DI8, 3PJ8, 2W4O, 2GDO, 2E9N, and 2C6O). (*D*) A cartoon representation of the ATP/NAF binding site in CIPK23ΔC T190D (*Upper*) and CIPK24/SOS2ΔC T168D (*Lower*). The positions of the residues around the cholate ring, in sticks, are roughly conserved in both structures, implying that the binding of the CHAPS molecule is not affecting the overall cavity conformation. (*E*) A surface representation of the CIPK23ΔC T190D and the activation loop interacting surface. The calculated CIPK23ΔC T190D surface area buried by the accessible moiety of the activation loop is 757 $Å^2$ (displayed in brown). The contribution of the cholate ring to this area is less than 6% through its interaction with Leu-187 and His-189 (1), suggesting that CHAPS binding does not affect the conformation of the activation loop, although it cannot be discarded local effects in the vicinity of Leu-187. The CHAPS molecule and Leu-187 and His-189 are represented in stick mode and the activation loop in a cartoon mode.

1. Hubbard SJ, Thornton JM (1993) NACCESS Computer Program (Department of Biochemistry and Molecular Biology, University College London, London).

Fig. S6. Ribbon representation of the structures of CIPK23ΔC T190D (*A*) and calcium/calmodulin-dependent protein kinase I (*B*) together with a surface representation of the cavity connecting the ATP binding site and the hinge region in CIPK23ΔC T190D. The calmodulin binding helix of the regulatory domain of the calcium/calmodulin-dependent protein kinase I overlaps with the CIPK23ΔC T190D cavity.

Fig. S7. (*A*) Alignment comparing the amino acid sequences of the junction region connecting the kinase and the regulatory domain of CIPKs. The sequences are divided in two groups: The upper group corresponds to CIPKs that include the two conserved hydrophobic residues and the CIPKs, and the lower group does not contain these two residues. Ser315 of CIPK23 and Ser294 of CIPK24/SOS2 are highlighted with a red arrow (1). (*B*) A temperature B-factors representation of CIPK23ΔC T190D structure. B factors describe the mobility of the atoms around their determined positions, thus they represent a measurement of the peptide chain flexibility. The structure is drawn in a cartoon representation, where the color is ramped by residue from blue, as the lowest B-factor value, to red, as the highest B-factor value. In addition, the size of the tube also reflects the value of the B factor, where the larger the B factor, the thicker the tube.

1. Hashimoto K, et al. (2012) Phosphorylation of calcineurin B-like (CBL) calcium sensor proteins by their CBL-interacting protein kinases (CIPKs) is required for full activity of CBL-CIPK complexes toward their target proteins. *J Biol Chem* 287(11):7956–7968.

Table S1. Data collection and refinement statistics

Data collection			
Construct	CIPK23	CIPK23 T190D	CIPK24/SOS2 T168D
Space group	$P2_12_12_1$	$P2_12_12_1$	P1
Cell dimensions			
a, b, c, Å	72.25, 91.46, 207.2	72.20, 91.73, 207.9	69.11, 71.35, 77.83
α, β, γ, °	90.0, 90.0, 90.0	90.0, 90.0, 90.0	104.8, 100.3, 118,9
Resolution, Å	59.26–2.30 (2.42–2.30)	49.97–1.90 (2.00–1.90)	70.2–3.3 (3.68–3.40)
R_{pim}	0.050 (0.335)	0.042 (0.362)	0.15 (0.68)
$CC_{1/2}$	0.996 (0.707)	0.997 (0.654)	0.994 (0.56)
I/σ(I)	12.8 (3.1)	12.8 (2.3)	5.7 (1.8)
Completeness, %	99.9 (99.9)	100.0 (100.0)	91.0 (93.1)
Redundancy	13.2 (12.4)	8.3 (8.3)	3.7 (3.7)
Refinement			
Resolution, Å	59.26–2.30 (2.38–2.30)	49.97–1.90 (1.97–1.90)	70.2–3.4 (3.49–3.40)
No. of reflections	61,816	110,291	13,859
$R_{\mathrm{work}}/R_{\mathrm{free}}$	17.3/22.7 (22.7/29.8)	19.2/23.3 (26.3/30.7)	26.6/27.4 (35.0/40.0)
No. of atoms			
Protein	9440	9394	8821
CHAPS	294	294	—
Sulfate ions	155	84	—
Water molecules	589	822	—
Average B factors	36.8	29.8	70.9
rmsd			
Bond lengths, Å	0.008	0.008	0.005
Bond angles, °	1.080	1.130	1.126
Ramachandran plot	95.0% in the core 5.0% in the allowed	97.0% in the core 3.0% in the allowed	96.0% in the core 4.0% in the allowed

Highest-resolution shell is shown in parentheses.

$R_{pim} = \frac{\sum_{hkl}\sqrt{\frac{1}{n-1}}\sum_{j=1}^{n}\left|I_{hkl,j} - \langle I_{hkl}\rangle\right|}{\sum_{hkl}\sum_{j}I_{hkl,j}}.$

Table S2. Primer sequences

Primer name	Primer type	Sequence 5′→3′
23N	Forward	GGAATTCCATATGGGTAGGACACGAG
23N2	Forward	AACCCGGGAATGGCTTCTCGAACAACG
23C	Reverse	AGGATGCGGCCGCTCATACTGGTGTTTTG
23T190D5	Forward	GTTACTTCACGATACCTGTGGAACA
23T190D3	Reverse	TGTTCCACAGGTATCGTGAAGTAAC
23V182K5	Forward	CCTCAGCAAAAACGAGAGGATGGG
23V182K3	Reverse	CCCATCCTCTCGTTTTTGCTGAGG
23S176D5	Forward	GACTTTGGATTGGACGCTCTACCTCAGCAAG
23S176D3	Reverse	CTTGCTGAGGTAGAGCGTCCAATCCAAAGTC
23Y197E5	Forward	GGAACACCCAATGAAGTTGCTCCGGAGG
23Y197E3	Reverse	CCTCCGGAGCAACTTCATTGGGTGTTCC
23I308DF309D5	Forward	GCCTTGATGATGTTGATGCAGACGATGATGACTCAGGGGAGTC
23I308DF309D3	Reverse	GACTCCCCTGAGTCATCATCGTCTGCATCAACATCATCAAGGC
23SOS2like5	Forward	CCTCAGCAAGGTGTAGAGTTACTTCGCACAACCTGTGGAACACCC
23SOS2like3	Reverse	CCACAGGTTGTGCGAAGTAACTCTACACCTTGCTGAGGTAGAGCGC
24N	Forward	CGGGATCCATGAGAAGAGTGGGCAAG
24C	Reverse	CGGAATTCTCACAGGGGCCCTTCATCATTTCTCTC
24T168D5	Forward	GAGTAGAACTTCTGCGTGACACATGTGG
24T168D3	Reverse	CACATGTGTCACGCAGAAGTTCTACTCC
24S228D5	Forward	GCAGAGTTTGATTGTCCACCGTGGTTTTCC
24S228D3	Reverse	GGAAAACCACGGTGGACAATCAAACTCTGC
24E107KS109D5	Forward	GGAGGCTTAAAGAAGATGAGTCTCGGAAATAC
24E107KS109D3	Reverse	GACACATCTTCTTTAAGCCTCCCTTTATGAAC
24C127S5	Forward	CATTGTCACAGCAAGGGTGTTTACCAC
24C127S3	Reverse	CCTTGCTGTGACAATGAGCAACAG
24P81K5	Forward	GGCGAGTAAGTCGAAAATATATATAGTTTTGG
24P81K3	Reverse	CAGAAAAAATTATGTGCCTATACGAGCAAG
24L266K5	Forward	TTCGACTTACTCGCCAACACCTC
24L266K3	Reverse	CACATAATTTTTTCTGAACCAAGGATCTTTC
23FN	Forward	CCATCATCACCACAGCCAGGATCCGGGTAGGACACGAGTTGGTAAG
23FC	Reverse	GCATTATGCGGCCGCAAGCTTTCATTCGAAAAGTGAACCGAGATTG
CBL1N	Forward	GGAATTCCATATGATGGGCTGCTTCCACTC
CBL1C	Reverse	GGGGTACCTCATGTGGCAATCTCATCG